Progress In Electromagnetics Research Letters, Vol. 90, 53–60, 2020

FDA Transmit Beamforming Synthesis Using Chebyshev Window Function Technique to Counteract Deceptive Electronic Countermeasures Signals

Shaddrack Y. Nusenu[1, *], Abdul Basit[2], and Emmanuel Asare[1]

Abstract—Frequency diverse array (FDA) has gained remarkable attention in both radar and communication applications over the years due to its unique range-dependent beamforming. On the other hand, extremely less attention is paid to the exploitation of FDA in electronic countermeasures (ECM). Hence, this paper proposes a symmetric frequency diverse array via Chebyshev window function in ECM applications. Specifically, we utilize Chebyshev window function to design the coefficient of both transmit weights and frequency diverse increments to uncouple range-angle response of the true target to counteract deceptive ECM signals. In addition, we consider a real constraint scenario, i.e., the propagation of the electromagnetic signal arriving at the true target position. The attribute of the proposed scheme is that it is able to discriminate between true target location and false target(s) location. This implies that the generated false target(s) by the jammer can be suppressed significantly in either angular or range profile mismatch. Further, we adopt Swerling 1 model to devise generalized Neyman-Pearson design rule to evaluate the probability of detection of the proposed scheme. Numerical results illustrate the achievements of the proposed scheme.

1. INTRODUCTION

Phased-arrays (PA) are commonly employed in many applications, especially in modern communications, radar, and navigation systems [1–3]. The directional gain of the PA is able to detect or track weak targets along pre-specified direction while suppressing strong sidelobe interferences along other directions. Therefore, the utilization of PA has gained massive support in the past years in both military radar and civilian applications. Nevertheless, with technological advancement of military radar, electronic countermeasures (ECM) has emerged rapidly posing threat to PA antenna technology [4]. The PA beamforming is angle-dependent only (i.e., for all the range cells, it is fixed at a particular angle). This implies that it cannot estimate range-dependent targets as a result of inherent range ambiguity [5].

Recently, radar systems face more challenging tasks in electronic warfare ECM applications, particularly, using deceptive signals/jamming [6–8]. The main object of the deceptive ECM is to generate deceptive signals to confuse/disrupt the radar system from detecting and/or tracking the true target(s) from the false ones.

Over the past years, digital radio frequency memory (DRFM) technology [9, 10] has been utilized to prevent hostile radar systems from achieving its deceptive purposes. However, it is realized that different jamming may cause serious degradation to the radar sensing performance. From the above contexts, it has become necessary for the modern radar systems to devise techniques with distinct advantages in the electronic counter countermeasure (ECCM).

Received 10 December 2019, Accepted 11 January 2020, Scheduled 5 March 2020

* Corresponding author: Shaddrack Yaw Nusenu (nusenu2012gh@yahoo.com).

[1] Koforidua Technical University (KTU), Ghana. [2] International Islamic University, Islamabad, Pakistan.

Numerous researches have worked on ECCM primarily focusing on combating deceptive jamming [11–16]. According to the authors' knowledge, only a few works are reported in ECCM applications using FDA technology, for instance [4, 17, 18] but ignore the propagation process of the radiated target signal. It should be mentioned that PA can be employed in ECCM applications. However, it is only angle dependent (i.e., 1-dimensional view). Therefore, there is a need to further investigate ECCM methods by exploiting the promising potentials of FDA (i.e., two-dimensional view range-angle beamforming).

Current works on FDA mainly focus on radar and communication applications, for instance [19–31]. Considering the extremely limited literature on FDA technology in ECCM applications, we propose Chebyshev window function to compute both the frequency diverse increment and transmit weights along symmetric array elements to counteract deceptive ECM signals. Taking the real constraint scenario into account, (i.e., propagation of the electromagnetic signal arriving at the true target position), we can discriminate between the true target and false target(s). Thus, the generated false targets by the jammer can be suppressed in either angular or range profile mismatch. We analyze SINR using minimum variance distortionless response (MVDR). In addition, we utilize generalized Neyman-Pearson rule to design multiple hypotheses to detect the true target detection from the false target(s), noises, and interferences. Herein, we adopt Swerling 1 model (i.e., target's statistical features have time variations).

The rest of the paper is organized as follows. Section 2 presents symmetrical FDA Chebyshev window function technique. In Section 3, analysis of interference and deceptive jamming signals suppression is provided. Section 4 gives the performance evaluation. Section 5 provides simulation results, and finally, conclusions are drawn in Section 6.

2. SYMMETRICAL FDA CHEBYSHEV WINDOW FUNCTION TECHNIQUE

Consider the symmetrical FDA geometry shown in Fig. 1 with odd number of elements $P = 2N + 1$. The radiation frequency $f_n(t)$ is determined as [30]

$$f_n = f_0 + \Delta f_n; \quad -N \leq n \leq N \tag{1}$$

and the nonuniform frequency diverse increment is $\Delta f_n = \beta_n \Delta f$, with β_n being the nth element coefficient computed by Chebyshev window function [32]. The benefits of using Chebyshev window-based tapering are: 1), simple computation, 2) enhanced sidelobe levels suppression, and 3) produces sharp mainlobe towards the true target location. The proposed frequency diverse increment Δf_n is written in Eq. (2)

$$\Delta f_{N-n} = \Delta f \left\{ \frac{\cos\left(P\cos^{-1}\left[\Upsilon \cos\left(n\pi/P\right)\right]\right)}{\cosh\left(P\cosh^{-1}\left(\Upsilon\right)\right)} \right\}; \quad n = 0, 1, \ldots, 2N \tag{2}$$

where $\{\cdot\}$ is a general Chebyshev window equation and $\Upsilon = \cosh[(P)^{-1}\cosh^{-1}(10^{\varepsilon})]$ with ε utilized to control the sidelobes level in the true target coverage area. The corresponding symmetrical FDA array

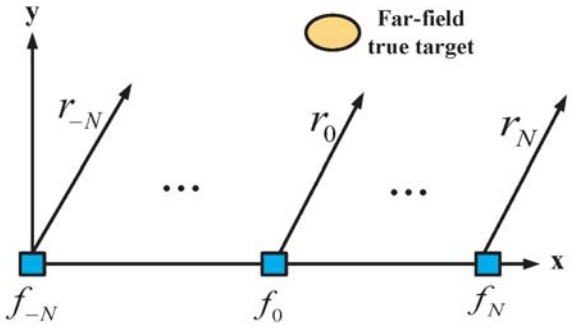

Figure 1. Standard FDA antenna geometry.

factor is given in Eq. (3), where $r_n = r - nd\sin\theta$ denotes the target range from the nth element; θ is the direction; and c is the light speed.

$$AF(\theta, r, t) = \sum_{n=-N}^{N} w_{T,n} \exp j\left[2\pi f_n\left(t - \frac{r_n}{c}\right) \cdot \left(t - \frac{r_n}{c}\right)\right] \tag{3}$$

Note that for the transmitted signal to arrive at the true target location (θ_0, r_0), we consider $t \in [\frac{r_0}{c}, T + \frac{r_0}{c}]$ with T being the pulse duration [31]. Referring to Eq. (3), we can rewrite the symmetrical FDA transmit beamforming as

$$\tilde{B}_{FDA}(\theta, r, t) = \left| \sum_{n=-N}^{N} w_{T,n} \exp\left\{j\frac{2\pi f_0 nd\sin\theta}{c}\right\} + \exp\left\{j2\pi\beta_n\Delta f\left(t - \frac{r_n}{c}\right) \cdot \left(t - \frac{r - nd\sin\theta}{c}\right)\right\}\right|^2 \tag{4}$$

It should be noted that the weighting vector $w_{T,n}$ in Eq. (4) can be designed to synthesis the desired transmit beampattern. Hence, we employ Chebyshev window function to compute the $w_{T,n}$ given in Eq. (5)

$$w_{T,N-n} = \left\{\frac{\cos\left(P\cos^{-1}\left[\tilde{\Upsilon}\cos\left(n\pi/P\right)\right]\right)}{\cosh\left(P\cosh^{-1}\left(\tilde{\Upsilon}\right)\right)}\right\}; \quad n = 0, 1, \ldots, 2N \tag{5}$$

where $\tilde{\Upsilon} = \cosh[(P)^{-1}\cosh^{-1}(10^{\varepsilon_1})]$, with ε_1 used to control the sidelobes level for the weights. It is important to note that ε and ε_1, respectively, can be used to regulate the sidelobes levels appropriately to provide more degrees of freedom for the proposed scheme.

3. ANALYSIS OF INTERFERENCE AND DECEPTIVE JAMMING SIGNALS SUPPRESSION

One of the main object of the radar system is to obtain the true target information, especially in a coverage scenario free from jammers or multiple interference sources. In case a radar system is jammed, the jamming signals suppress the desired target signals. Thus, erroneous information may be obtained. Therefore, there is a need for the radar system to devise methods to precisely estimate and/or distinguish between true target signals and false signals. In this section, interference and jamming signal characteristics are discussed.

Suppose that a true target is located at (θ_0, r_0). We also assume multiple interference sources at (θ_i, r_i) and repeated jammer generated false targets (θ_k, r_k). The received baseband signals at the receiver array are

$$\mathbf{x}(t) = \alpha_0\phi_0\mathbf{a}(\theta_0, r_0)\, s(t-\tau) + \sum_{i=1}^{D} \alpha_i\phi_i\mathbf{b}(\theta_i, r_i)\, s(t-\tau_i) + \sum_{k=1}^{K} \alpha_k\phi_k\mathbf{b}(\theta_k, r_k)\, s((t-t_k)-(t-\tau_k)) + \mathbf{v}(t) \tag{6}$$

where α_0, and α_i are the complex amplitudes of the desired target and the ith interference source, respectively, and α_k denotes the complex amplitude of the kth false target. (θ_k, r_k) is the kth false targets angular-range pair, t_k the observing time of the jammer, and τ_k the time delay of the jammer. $\mathbf{v}(t)$ is the noise term with σ_v^2 variance. ϕ_k, ϕ_0, and ϕ_i are a constant for a given kth false target, true target, and the ith interference source, respectively, and the receive steering vector is $\mathbf{b}(\theta, r)$.

In radar systems, the reflected signal is utilized to detect the presence of a target. Since the probability of detection is related to the signal-to-noise ratio (SNR), we employ a matched filter whose impulse response is determined by the transmitted signal in a way that will result in the maximum SNR at the output of the filter when that signal and noise are passed through the filter. Therefore, after matched filtering, it yields

$$\mathbf{y}(\tau) \triangleq \alpha_0\mathbf{u}(\theta_0, r_0) + \sum_{i=1}^{D} \alpha_i\mathbf{u}(\theta_i, r_i) + \sum_{k=1}^{K} \alpha_k\mathbf{u}(\theta_k, r_k) + \mathbf{v} \tag{7}$$

In Eq. (7), the first, second, third, and fourth terms on the right hand side represent the true target, interference sources, deceptive signals, and noise, respectively.

4. PERFORMANCE EVALUATION

4.1. Analysis of Signal-to-Interference-Plus-Noise Ratio (SINR)

We employ minimum variance distortionless response (MVDR) which can be expressed in the following optimization form:

$$\begin{aligned} &\min_{\mathbf{w}_R} \ \mathbf{w}_R^H \mathbf{R}_{i+v} \mathbf{w}_R \\ &s.t \ \mathbf{w}_R^H \mathbf{u}\left(\theta_0, r_0\right) = 1 \end{aligned} \tag{8}$$

where $\mathbf{w}_R$ is represented by received weight, and $\mathbf{R}_{i+v}$ denotes the covariance matrix representing the interference-plus-jamming-plus-noise which is given in Eq. (9) [33].

$$\hat{\mathbf{R}}_{i+v} = \sum_{i=1}^{D} \sigma_i^2 \mathbf{u}\left(\theta_i, r_i\right) \mathbf{u}^H\left(\theta_i, r_i\right) + \sum_{k=1}^{K} \sigma_k^2 \mathbf{u}\left(\theta_k, r_k\right) \mathbf{u}^H\left(\theta_k, r_k\right) + \sigma_v^2 \mathbf{I} \tag{9}$$

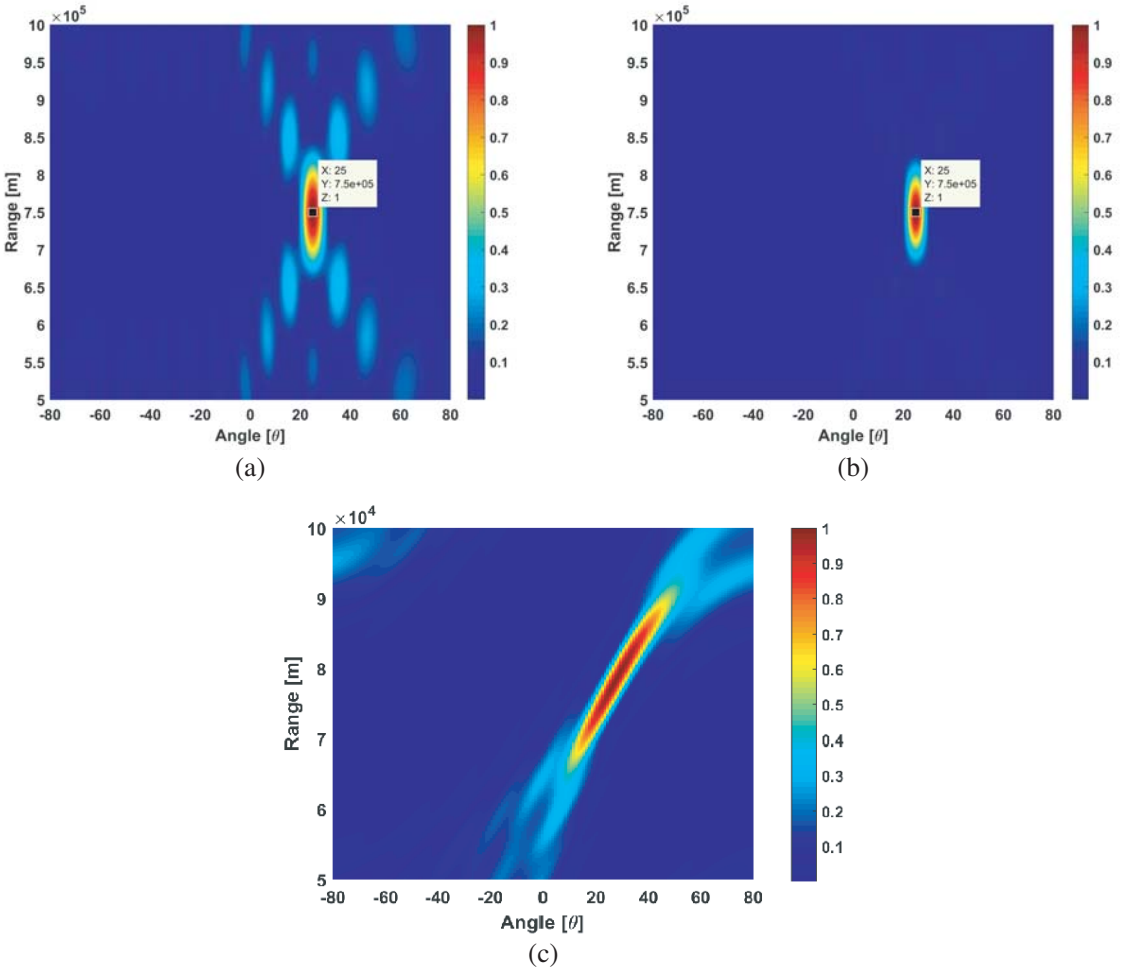

Figure 2. 2-dimensional range-angle beamforming illustrations: (a) Symmetrical FDA Chebyshev window function design for only time-dependent frequency increment at $t = 0.0025$ sec; (b) Symmetrical FDA Chebyshev window function design for both time-dependent frequency increment and transmit weight at $t = 0.0025$ sec; (c) log-FDA [35] for comparison purpose.

The output SINR of the proposed scheme can be evaluated as

$$SINR \triangleq \frac{\left|\mathbf{w}_R^H \mathbf{u}\left(\theta_0, r_0\right)\right|^2}{\mathbf{w}_R^H \hat{\mathbf{R}}_{i+v} \mathbf{w}_R} \tag{10}$$

4.2. True Target Probability of Detection

In order to evaluate the probability of detection performance, we describe the coverage region by devising multiple hypotheses taking into account Swerling 1 model. Then, we have the following forms:

$$\begin{cases} H_0 : \mathbf{y} = \mathbf{v} \\ H_1 : \mathbf{y} = \mathbf{w}_{T,n} \mathbf{a}\left(\theta_0, r_0\right) \otimes \mathbf{b}\left(\theta_0, r_0\right) + \mathbf{v} \\ H_2 : \mathbf{y} = \mathbf{z}_1 + \mathbf{v} \\ H_3 : \mathbf{y} = \mathbf{z}_2 + \mathbf{v} \end{cases} \tag{11}$$

where $\otimes$ denotes the Kronecker product, and $\mathbf{z}_1 = \sum_{i=1}^{D} \alpha_i \mathbf{u}\left(\theta_i, r_i\right)$ and $\mathbf{z}_2 = \sum_{k=1}^{K} \alpha_k \mathbf{u}\left(\theta_k, r_k\right)$, respectively, denote interference and deceptive ECM signals. The Neyman-Pearson rule can be analyzed from the likelihood ratio test [34] as

$$\Psi_1 = \log \frac{P_r\left(\mathbf{y}; H_1\right)}{P_r\left(\mathbf{y}; H_0\right)} \underset{H_1}{\overset{H_0}{\gtrless}} \xi \tag{12a}$$

$$\Psi_2 = \log \frac{P_r\left(\mathbf{y}; H_1\right)}{P_r\left(\mathbf{y}; H_2\right)} \underset{H_1}{\overset{H_2}{\gtrless}} \xi \tag{12b}$$

$$\Psi_3 = \log \frac{P_r\left(\mathbf{y}; H_1\right)}{P_r\left(\mathbf{y}; H_3\right)} \underset{H_1}{\overset{H_3}{\gtrless}} \xi \tag{12c}$$

where ξ represents the threshold for the true target detection. It should be noted that Eqs. (12a), (12b), and (12c) can be viewed as a unique permutation framework to test whether the true target exists or not in the coverage region.

5. SIMULATION RESULTS

The parameters for the simulation environment are: $f_0 = 10\,\text{GHz}$, $N = 15$, and $\Delta f = 30\,\text{kHz}$, true target position $(25^\circ, 750\,\text{km})$. The transmit weights and frequency increment values are computed via Chebyshev window function as shown in Fig. 1. The sidelobes level is fixed at $\varepsilon = \varepsilon_1 = 25\,\text{dB}$. Note that the wave propagation will arrive at the true target location at $t \in [0.0025\,\text{sec},\ 0.0035\,\text{sec}]$ and $T = 0.001\,\text{s}$.

In Fig. 2, we plot the transmitted beampatterns of our proposed FDA Chebyshev window function. More importantly, we compare frequency increment designed based on Chebyshev window function only with that of frequency increment and transmit weight based on Chebyshev window function, respectively shown in Fig. 2(a) and Fig. 2(b). We notice that both figures have focused beamforming towards the true target. Importantly, the beamforming in Fig. 2(b) outperforms the one in Fig. 2(a) in terms of sidelobe levels which has been suppressed significantly in the surveillance region. In Fig. 2(c), we show the log-FDA beamforming [35] for comparison purpose. It is evident that the beamforming of our proposed scheme outperforms log-FDA beamforming [35].

Fig. 3 depicts how the proposed scheme is able to distinguish between true target at $t = 0.0025\,\text{sec}$ and false target position $(25^\circ, 900\,\text{km})$ at $t = 0.003\,\text{sec}$. Note that the same angle direction but different ranges are assumed. As demonstrated in the figure, it is evidently clear that the proposed scheme has the potential in ECCM applications. Thus, true target can be differentiated from the false target(s) in the coverage region.

In plotting the output SINR, we consider the following: a true target with a fixed power of 12 dB, two generated false targets, namely, $(25^\circ, 900\,\text{km})$ and $(10^\circ, 600\,\text{km})$, with fixed power of 20 dB. Furthermore,

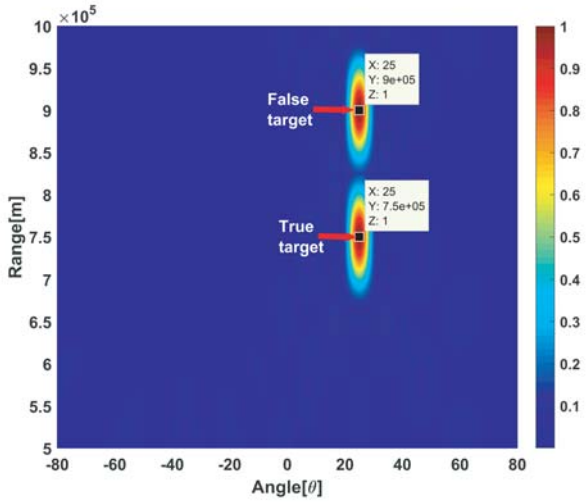

Figure 3. Discrimination between true target and false target beamforming in a given coverage region.

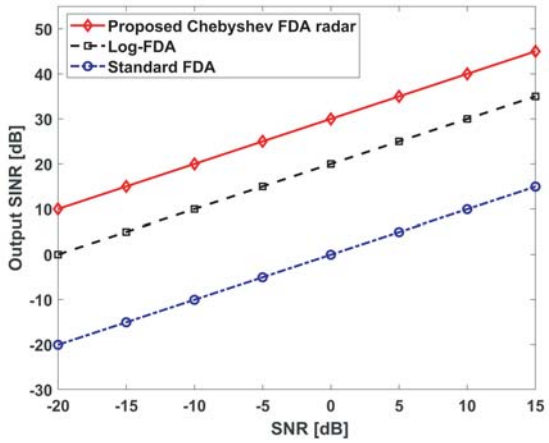

Figure 4. Output SINR performances with jamming ECM signals.

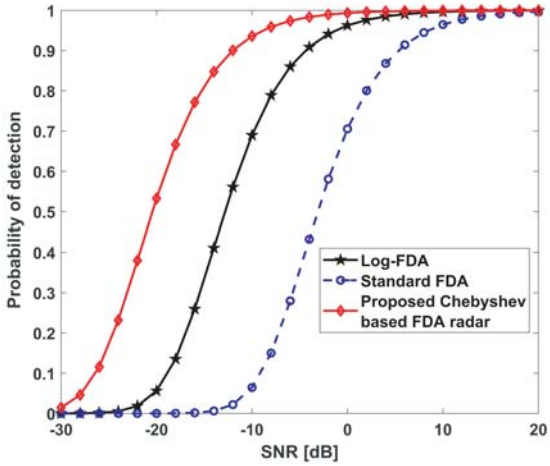

Figure 5. Detection curves performance with jamming ECM signals.

we assume that one interference is located at $(15°, 650\,\text{km})$ with interference power fixed at 15 dB. Fig. 4 depicts the performance of the output SINR versus signal-to-noise ratio (SNR). It can be noticed in the figure that in the presence of deceptive ECM signals, the proposed scheme outperforms log-FDA [35] and standard FDA. Also, the figure does indicate that the standard FDA performance is degraded significantly compared to log-FDA [35] because of the range-angle dependent coupling effect.

In Fig. 5, we evaluate the proposed Chebyshev based FDA radar detection performance and compared with other radar systems. Note that we adopt the same parameters used in Fig. 4. We also set the probability of false alarm $P_{fa} = 10^{-5}$. As shown in the figure, the proposed Chebyshev based FDA radar, log-FDA [35], and standard FDA show a satisfactory detection estimation performance. However, our proposed Chebyshev based FDA radar yields better results than the other two radar systems. This is because the proposed Chebyshev based FDA produces more focused transmitted energy towards the true target location. We notice that for a probability of detection (Pd) of 0.9, the proposed scheme, log-FDA, and standard FDA SNRs are around $-13\,\text{dB}$, $-5\,\text{dB}$, and $4\,\text{dB}$, respectively. This implies that the proposed Chebyshev based FDA radar has the ability to detect and estimate the true target information along range-angle domain if present.

6. CONCLUSION

This paper proposes a symmetrical FDA using Chebyshev window function to compute the coefficients of both transmit weights and frequency increments. In doing so, we can directly estimate the true target range-angle from the proposed symmetrical FDA Chebyshev window function peak output. In addition, we achieve a low sidelobe with its mainbeam focused in the true target range-angle location. With this unique advantage, the proposed scheme has the ability to counteract the deceptive ECM signals. Further, we design multiple hypotheses using Neyman-Pearson-based rule to detect the true target from the deceptive ECM signals, interference, and noise. The numerical results show that the proposed symmetrical FDA Chebyshev window function is very attractive in ECCM applications. In our subsequent work, we plan to investigate new detection algorithms to enhance the proposed detection scheme in ECCM applications.

REFERENCES

1. Wong, K. T., Y. I. Wu, Y. S. Hsu, and Y. Song, "A lower bound of DOA estimates by an array randomly subject to sensor-breakdown," *IEEE Sensors Journal*, Vol. 12, No. 5, 911–913, May 2012.
2. Giannoccaro, N. I. and L. Spedicato, "A new strategy for spatial reconstruction of orthogonal planes using a rotating array of ultrasonic sensors," *IEEE Sensors Journal*, Vol. 12, No. 5, 1307–1316, May 2012.
3. Yong, S. and J. T. Bernhard, "A pattern reconfigurable null scanning antenna," *IEEE Transactions Antennas Propagation*, Vol. 60, No. 10, 4538–4544, Oct. 2012.
4. Ahmed, A., W. Q. Wang, Z. Yuan, et al., "Subarray-based FDA radar to counteract deceptive ECM signals," *EURASIP Journal on Advances in Signal Processing*, 1–11, 2016, DOI 10.1186/s13634-016-0403-6.
5. Wang, W. Q., "Mitigating range ambiguities in high PRF SAR with OFDM waveform diversity," *IEEE Geoscience Remote Sensing Letters*, Vol. 10, No. 1, 101–105, Jan. 2013.
6. Poisel, R. A., *Information Warfare and Electronic Warfare Systems*, Artech House, Norwood, MA, USA, 2013.
7. Liu, N. J. and Y. T. Zhang, "A survey of radar ECM and ECCM," *IEEE Transactions Aerospace Electron Systems*, Vol. 31, No. 3, 1110–1120, Jul. 1995.
8. Farina, A., "Electronic counter-countermeasures," *Radar Handbook*, 3rd edition, M. Skolnik (ed.), McGraw-Hill, New York, NY, USA, 2008.
9. Roome, S. J., "Digital radio frequency memory," *Electronics and Communication Engineering Journal*, Vol. 2, No. 4, 147–153, Aug. 1990.
10. Berger, S. D., "Digital radio frequency memory linear range gate stealer spectrum," *IEEE Transactions Aerospace Electron Systems*, Vol. 39, No. 2, 725–735, Apr. 2003.
11. Akhtar, J., "Orthogonal block coded ECCM schemes against repeat radar jammers," *IEEE Transactions Aerospace Electron Systems*, Vol. 45, No. 3, 1218–1226, 2009.
12. Zhang, J., D. Zhu, and G. Zhang, "New antivelocity deception jamming technique using pulses with adaptive initial phases," *IEEE Transactions Aerospace Electron Systems*, Vol. 49, No. 2, 1290–1300, 2013.
13. Rao, B., S. Xiao, X. Wang, and T. Wang, "Maximum likelihood approach to the estimation and discrimination of exoatmospheric active phantom tracks using motion features," *IEEE Transactions Aerospace Electron Systems*, Vol. 48, No. 1, 794–819, 2012.
14. Coluccia, A. and G. Ricci, "ABORT-Like detection strategies to combat possible deceptive ECM signals in a network of radars," *IEEE Transactions Signal Processing*, Vol. 63, No. 11, 2904–2914, 2015.
15. Bandiera, F., A. Farina, D. Orlando, and G. Ricci, "Detection algorithms to discriminate between radar targets and ECM signals," *IEEE Transactions Signal Processing*, Vol. 58, No. 12, 5489–5993, 2010.

16. Greco, M., F. Gini, and A. Farina, "Radar detection and classification of jamming signals belonging to a cone class," *IEEE Transactions Signal Processing*, Vol. 56, No. 5, 1984–1993, 2008.
17. Xu, J., G. Liao, S. Zhu, and H. C. So, "Deceptive jamming suppression with frequency diverse MIMO radar," *Signal Processing*, Vol. 113, 9–17, 2015.
18. Gang, L., H. Huang, and W. Q. Wang, "Frequency diverse array radar in counteracting mainlobe jamming signals," *2017 IEEE Radar Conference (RadarConf)*, 1228–1232, 2017.
19. Nusenu, S. Y., Z. Wang, and W. Q. Wang, "FDA radar using Costas sequence modulated frequency increments," *2016 CIE International Conference on Radar*, 1–4, Oct. 10–13, 2016, DOI:10.1109/RADAR.2016.8059332.
20. Nusenu, S. Y., W. Q. Wang, and A. Basit, "Time-modulated FD-MIMO array for integrated radar and communication systems," *IEEE Antennas and Wireless Propagation Letters*, Vol. 17, No. 6, 1015–1019, Jun. 2018.
21. Nusenu, S. Y. and W.-Q. Wang, "Dual-function FDA MIMO radar-communications system employing costas signal waveforms," *2018 IEEE Radar Conference (RadarConf)*, 0033–0038, 2018.
22. Nusenu, S. Y., H. Shao, P. Ye, et al., "Dual-function radar-communications system design via sidelobe manipulation based on FDA Butler matrix," *IEEE Antennas and Wireless Propagation Letters*, Vol. 18, No. 3, 452–456, Mar. 2019.
23. Nusenu, S. Y. and A. Basit, "Cognitive transmit subarray FDA design for integrated radar-communication using flexible sidelobe control," *2018 IEEE 7th International Conference on Adaptive Science and Technology (ICAST)*, 1–6, 2018.
24. Nusenu, S. Y., W.-Q. Wang, and J. Xiong. "Time-modulated frequency diverse array for physical-layer security," *IET Microwaves, Antennas and Propagation*, Vol. 15, No. 3, 336–345, Apr. 2017.
25. Nusenu, S. Y., W. Q. Wang, and S. Ji, "Secure directional modulation using frequency diverse array antenna," *IEEE Radar Conference (RadarConf)*, 378–382, Seattle, WA, May 2017.
26. Nusenu, S. Y., H. Chen, W.-Q. Wang, S. Ji, and O. A. K. Opuni-Boachie, "Frequency diverse array using Butler matrix for secure wireless communications," *Progress In Electromagnetics Research M*, Vol. 63, 207–215, 2018.
27. Nusenu, S. Y. and W. Q. Wang, "Range-dependent spatial modulation using frequency diverse array for OFDM wireless communications," *IEEE Transactions Vehicular Technology*, Vol. 67, No. 11, 10886–10895, 2018.
28. Nusenu, S. Y. and A. Basit, "Frequency diverse array antennas: From their origin to their application in wireless communication systems," *Journal of Computer Networks and Communications*, 1–12, Article ID 5815678, 2018, https://doi.org/10.1155/2018/5815678.
29. Nusenu, S. Y., "Development of frequency modulated array antennas for millimeter–wave communications," *Wireless Communications and Mobile Computing*, Vol. 2019, 1–15, Article ID 6940708, 2019, doi.org/10.1155/2019/6940708.
30. Chen, K., S. Yang, Y. Chen, and S.-W. Qu, "Accurate models of time invariant beampatterns for frequency diverse array," *IEEE Transactions on Antennas and Propagation*, 1–1, 2019, DOI: 10.1109/TAP.2019.2896712.
31. Chen, B., X. Chen, Y. Huang, and J. Guan, "Transmit beampattern synthesis for FDA radar," *IEEE Antennas and Wireless Propagation Letters*, Vol. 17, 98–101, Jan. 2018.
32. Dolph, C. L., "A current distribution for broadside arrays which optimizes the relationship between beam width and side-lobe level," *Proceedings of the IRE*, Vol. 34, 335–348, 1946.
33. Van, H. L. T., *Optimum Array Processing*, Wiley, New York, 2002.
34. Wang, W. Q. and H. C So, "Range-angle localization of targets by a double-pulse frequency diverse array radar," *IEEE Journal Selected Topics Signal Processing*, Vol. 8, No. 1, 106–114, 2014.
35. Khan, W., I. M. Qureshi, and S. Saeed, "Frequency diverse array radar with logarithmically increasing frequency offset," *IEEE Antennas Wireless Propagation Letters*, Vol. 14, 499–502, 2015.